Failure analysis of shot–sleeves used in brass high pressure die–casting process

Dorra Abid[a], Ahmed Ktari[a,b,*], Dhouha Mellouli[a], Nedia Gafsi[a], Nader Haddar[a]

[a] Laboratoire de Génie des Matériaux et Environnement, LGME, ENIS, B.P. 1173–3038, Université de Sfax, Tunisia
[b] Laboratoire MSMP – EA7351, Arts et Métiers ParisTech, Aix-en-Provence, France

A R T I C L E I N F O

Keywords:
Shot sleeve
Damage assessment
Thermal fatigue
Crack growth
Shielding effect

A B S T R A C T

A failure investigation has been conducted on a two cases of shot-sleeve used in brass–die casting and made up of AISI H10 tool steels to study their failure mechanisms. The chemical composition of the shot–sleeves material and the hardness profiles were evaluated. A preliminary examination of shot–sleeves reveal the presence of cracks network on their inner surfaces which proves that thermal fatigue was probably the main cause of their failure. A Meticulous investigation of these damaged surfaces reveal the presence of an additional small zone cited in the vicinity of the plunger entry side. This zone presents several scratches sign of abrasive wear. Then, the measurement of the cracks length and their linear density along longitudinal and transversal cuts of the damaged shot–sleeve sample are carried out. Results show that the observed cracks network can be divided into two zones. The first one was the most damaged in terms of cracks density and length given that it is the first zone which enter in contact with the molten metal. However, the cracks network examined in the second zone appears to be superficial.

1. Introduction

The high pressure die-cast process is used to produce parts mostly from aluminium, magnesium, zinc and copper alloys by injection of the molten metal in the mold cavity. Parts produced by this process conform accurately to the die size, have favourable mechanical features, and are low in cost. Hence, this process has a wide range of application fields including the aircraft and automobile industries. During hot forming operations the tools steel used to this process are exposed to a sever thermal and/or mechanical loads which can lead to their damage. The improvement of these structures lifetime was strongly required due to several economic and environmental reasons. One of the major damage mechanisms occurring in hot forming tool steels, under cyclic thermal loads (*e.g.* die casting and forging [1–4]), is the formation of a network of interconnected cracks, often named *Heat–Checking* [5–8]. The stress cracking, which presents another variant of thermal fatigue cracks, was clearly marked in areas exposed to local stress concentrations and can lead to crack initiation in a die casting mold [9]. Then, these cracks can grow and became more pronounced driven by several factor including thermal fatigue, erosion, oxidation, soldering of the metal to the die surface, deformation of die contact surfaces and dangerous fracture [10–13].

In hot metal forming applications like stamping or die casting the service life time of the tools are limited due to their extreme working conditions in term of thermal and/or mechanical loads which result from the close contact between the tools and the hot work piece. In these applications the tools temperature can reach 1200 °C [13] when the molten metal attain 675 °C and 930 °C for Al–alloy casting and Cu–alloy casting respectively [14].

* Corresponding author at: Laboratoire de Génie des Matériaux et Environnement, LGME, ENIS, B.P. 1173–3038, Université de Sfax, Tunisia.
E-mail address: ahmed.ktari@enis.tn (A. Ktari).

https://doi.org/10.1016/j.engfailanal.2019.05.038
Received 7 April 2018; Received in revised form 22 May 2019; Accepted 30 May 2019
Available online 04 June 2019
1350-6307/

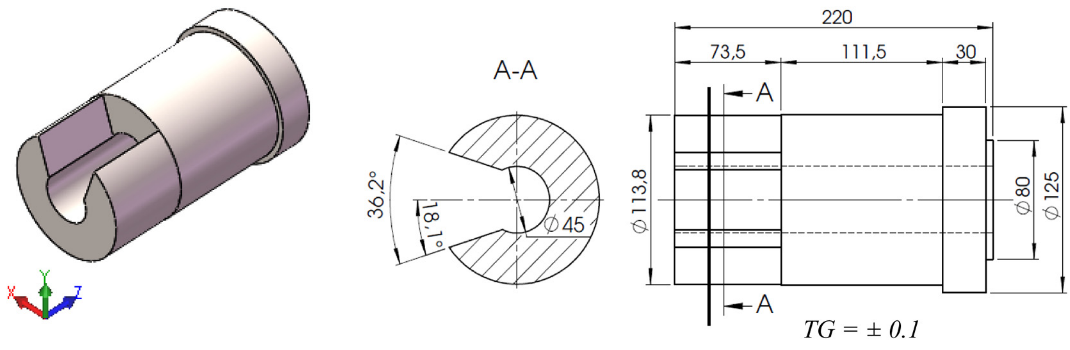

(a) 3D isometric view *(b) Dimensions (in mm)*

Fig. 1. Geometry and dimensions of the studied shot–sleeves.

Table 1
Process parameters in high pressure brass die–casting case of study.

Shot–sleeve filling	*2.5 s*
Injection phase	*0.1 s*
Cooling phase	*27 s*
Compression	*4 s*
Ejection and mold coating	*23 s*
Molten metal temperature	*950 °C*
Cast ejection temperature	*300 °C*

Table 2
Chemical composition of the studied material and usual steels grades used in hot work tools (% in weight).

	C	Si	Mn	P	S	Cr	Mo	V
Studied material	0.304	0.242	0.303	0.025	0.005	2.89	2.71	0.61
AISI H10	0.28–0.35	0.1–0.4	0.15–0.4	0–0.03	0–0.02	2.7–3.2	2.5–3.0	0.4–0.7
AISI H13	0.35–0.42	0.8–1.2	0.25–0.5	0–0.03	0–0.02	4.8–5.5	1.2–1.5	0.85–1.15

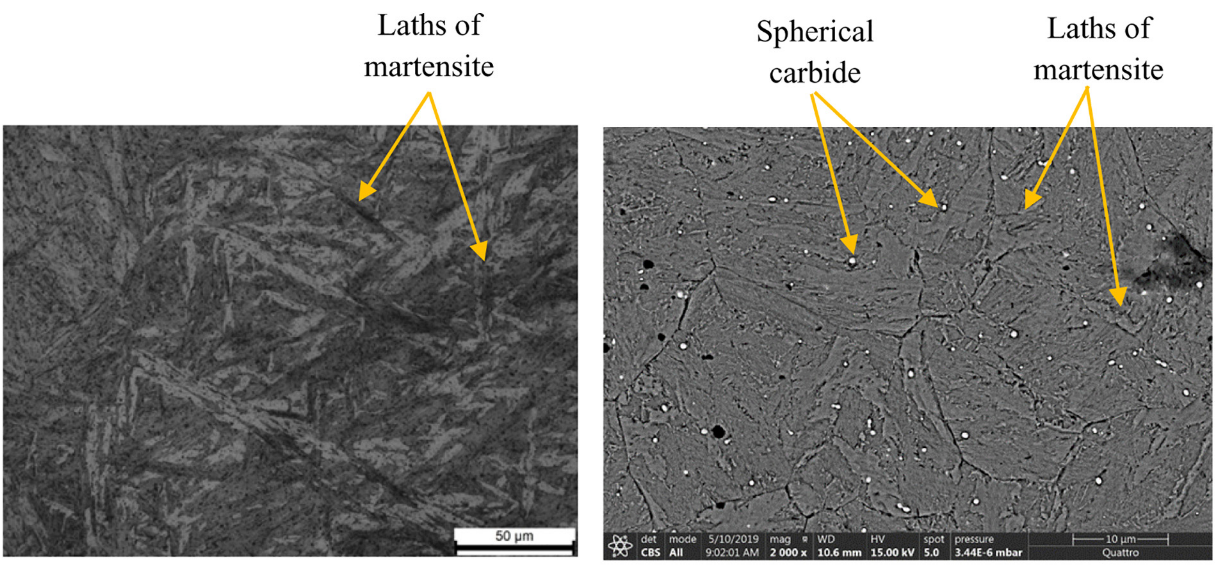

(a) *(b)*

Fig. 2. Microstructure of the shot-sleeve: (a) Light Optical Microscopy (LOM), (b) The SEM microanalysis.

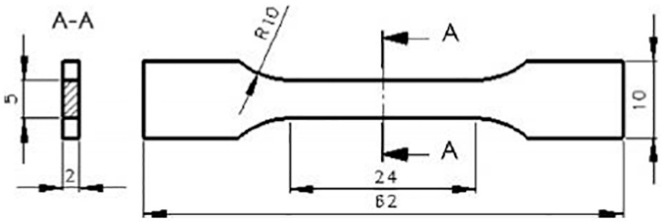

Fig. 3. Dimensions of tensile specimen (in mm).

Table 3
Monotonic mechanical properties of AISI H10 steel grade at room temperature.

Young's modulus [*GPa*]	Poisson's ratio	Yield strength $R_e[MPa]$	Tensile strength $R_m[MPa]$	A%
220	0.3	1580	1720	0.28

Under such working conditions, the tools are generally damaged through wear and thermal fatigue cracking processes [15–18]. Ktari et al. [19] have investigated a diesel engine crankshafts fracture used in train. Mellouli et al. [20] have investigated the thermal fatigue failure of a prematurely failed brass die-casting.

To improve the structures lifetime several researches have been conducted to study the effect of surface coatings on those structure lives. Panjan et al. [12] have studied the effect of duplex treatment composed of plasma nitriding and the deposition of 4-mm-thick PVD CrN coating on die-casting tools. They have found that wear of duplex treated tool is smaller than wear of the plasma nitrided tool. In addition, Srivastava et al. [21] have studied the effect of three-layer coating architecture on die surface: the outer layer consists of a thermal barrier coating composed of rare-earth oxide, the middle one is a TiAlN diffusion barrier coating and the inner layer is a thin adhesive Ti layer. These authors have found that this coating can significantly improves the thermal fatigue resistance of the substrate. Klobčar et al. [22] have studied the effect of cladding with maraging steels; they have found that this treatment provides good thermal fatigue resistance to the treated metal. The functionally graded materials (FGM) were also applied as a solution to improve the structure lifetime. Fazarinc et al. [23] have studied several FGM surfaces by changing amounts of alloying elements, precisely Si and Mo, they have found that their resistance to thermal fatigue is estimated at 27 times more resistant than the basic material.

In our case of study, two failed structures named shot–sleeve have been examined. This structure is a part of the die–casting injection press sited on the fixed mold side between the injection plunger and the sprue bush. In service, during the hot forming operations, the shot–sleeve undergo severe cyclic thermal–mechanical loads (*i.e.* the alternating of compressive and tensile stresses at the surface that arise from differential thermal expansion / contraction during sudden transient temperature changes [15,24]) which can lead to cracks initiation and propagation. The investigation of the thermo–mechanical fatigue shot sleeve was conducted according to the following points:

- Chemical and mechanical characterization of the shot sleeve material.
- Analysis of the failed zones to understand the main causes and mechanisms leading to the shot sleeve structures.

2. Shot sleeve materials characterization

In the present study, samples of shot–sleeve failed in service, were investigated to understand the mechanisms, which can lead to their damage. The shot–sleeve (Fig. 1), used in brass high pressure die–casting process, undergoes a severe thermo–mechanical loadings during cast cycles. Each cycle include principally four phases as following:

(i) The filling of the shot sleeve with the molten metal by means of a ladle,
(ii) The plunger moves through the shot–sleeve and press the casting material into the mold,
(iii) The cooling phase begin once the mold has been filled with molten metal and keep on until the casting cold. During the first part of this phase, named compression, a pressure is applied to the cooling metal by means of the plunger until the alloy has solidified.
(iv) The mold is then opened and the casting is removed with the ejector pins and the internal surfaces of the mold are sprayed with a lubricant before every cycle.

After the casting has been removed and the lubricant applied to the mold surfaces, the die are clamped together again then the cycle will repeat itself. The high pressure brass die–casting process parameters are summarized Table 1.

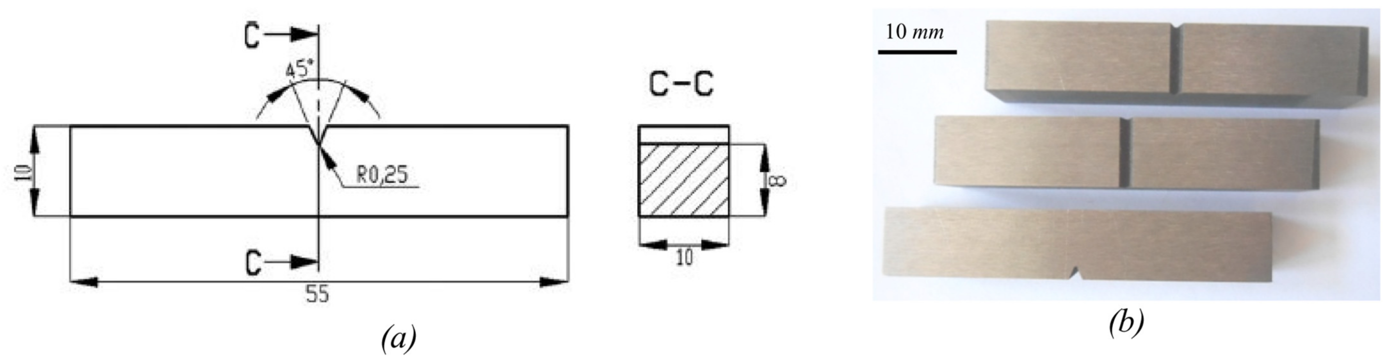

Fig. 4. Charpy V-notch specimens: (a) Geometry and dimensions (in mm), (b) machined Charpy V-notch specimens.

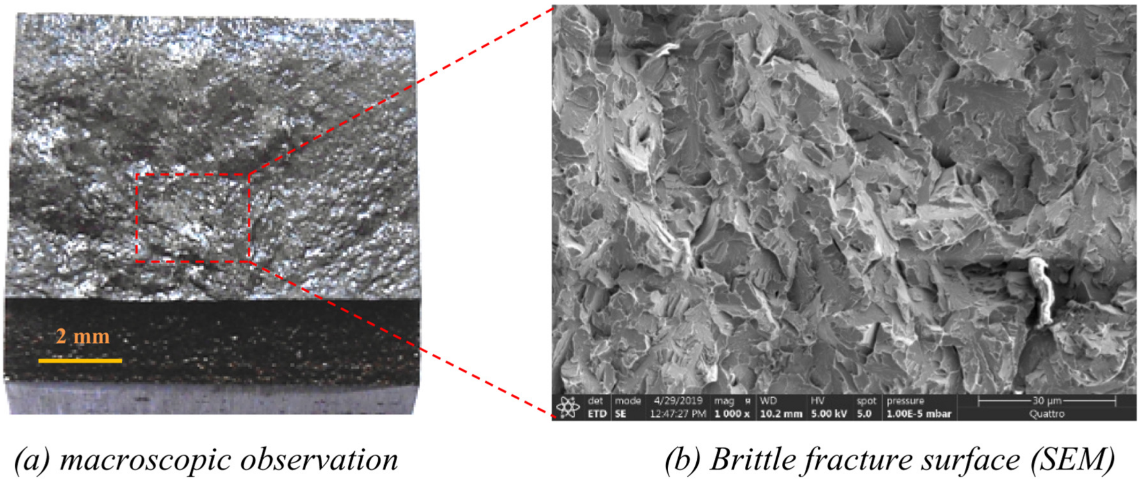

Fig. 5. Fracture surface of Charpy specimen. (a) macroscopic observation, (b) binocular microscope observation.

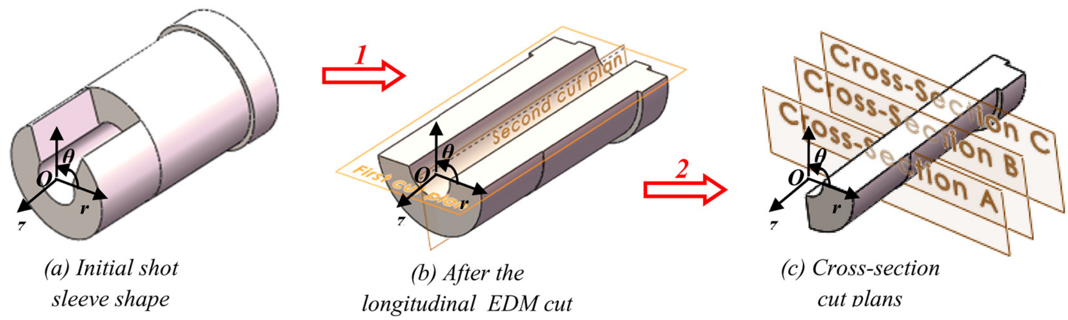

Fig. 6. CAO schema of shot–sleeve cutting planes: (a) Initial shot sleeve shape, (b) After the longitudinal EDM cut, (c) Cross-section cut plans.

2.1. Chemical analysis and microstructure

The chemical analysis of a sample of steel taken from damaged shot–sleeve was determined by means of a spectrometer (*Jobin Yvon JY 48®*). The typically steel grades used for hot work tools and our studied material are summarized in Table 2.

Materials used in high pressure die–cast process equipments have to combine a multitude properties to resist production constraints that they face. According to Reynoldson [25], a good material need to have: *(i)* low chemical reactivity with the surrounding environment (molten metal and oxygen), *(ii)* low thermal expansion and high thermal conductivity coefficients, *(iii)* high tempering resistance and *(iv)* a good toughness.

Both steel grades H10 (32CrMoV12–28) and H13 (X40CrMoV5–1) possess good resistance to abrasive effects, low sensibility to thermal shocks and good dimensional stability. However, H10 presents relatively high wear resistance compared to AISI H13 steel grade. The contents in chromium, molybdenum and vanadium give good hardenability, wear resistance, fracture toughness and hardness properties at high temperatures [26]. The chromium increases the hardenability of the steel, decreases the grain growth during austenitization, delay the softening during the tempering and contribute to the reduction of the high–temperature oxidation [27]. The molybdenum slows down the steel softening and give it a very good wear resistance at high temperature through the presence of hard metallic carbides M_6C and M_2C with a hardness of 1500 and 2000 HV respectively [27]. The vanadium allows to generate a very high carbides hardness (MC ≈ 3000 HV). It added generally, with a small amount, with chromium, molybdenum and tungsten to avoid the harmful oxidation resistance beyond 600 °C. The decrease of corrosion resistance is compensated by the presence of chromium [27].

Our studied material is H10, a metallographic observations were realized by means of an optical microscope (Leica®) on the same taken sample polished until mirror state then attacked by Nital (5% of nitric acid diluted in methanol). These observations show the presence of a martensitic structure (Fig. 2).

2.2. Mechanical properties

2.2.1. Tensile properties

In order to investigate the tensile properties of the studied material AISI H10, tensile tests were carried out on a three standard flat tensile specimens (NF A 03–151) as presented in Fig. 3. The semi–finishing form of each one was obtained from the damaged

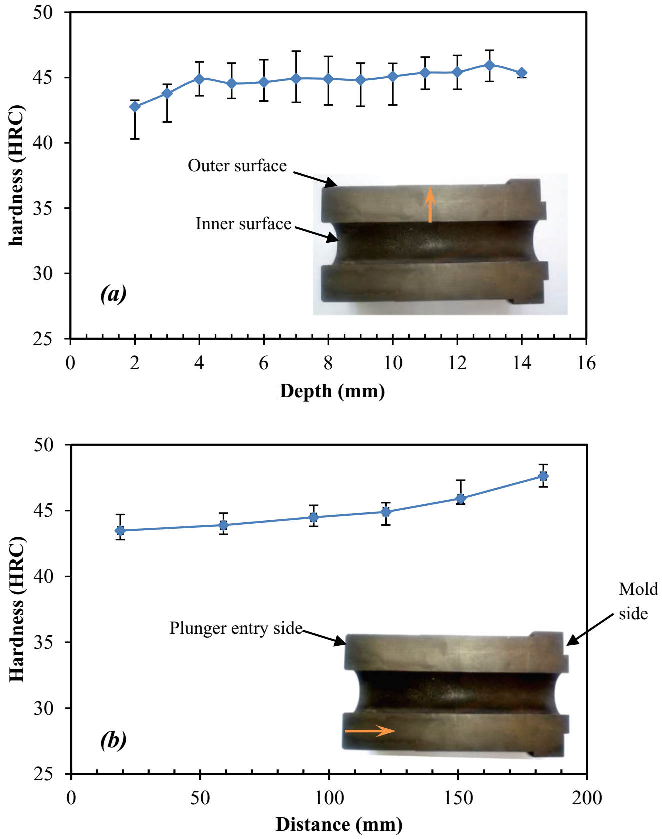

Fig. 7. Hardness shot–sleeve profiles, (a) from the entry to the mold zones, (b) from inner to the outer surfaces.

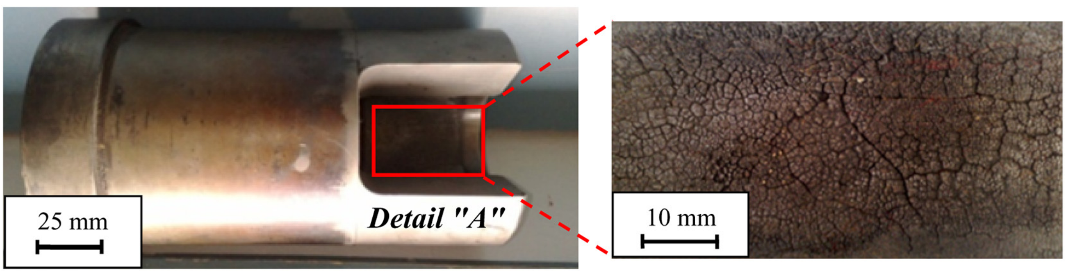

Fig. 8. Cracks network observed on the inner surface of the damaged shot–sleeve.

shot–sleeve case using a wire EDM machine. Then, specimens flat surfaces were mechanically grinding to obtain a good surface finish. These tests were conducted on a universal testing machine with capacity of *50 kN* and a crosshead speed of *0.5 mm/s*. The obtained results average are summarized in

Table 3.

2.2.2. The material toughness

Standard Charpy V-notched specimens were machined from the failed shot-sleeve by a wire EDM machine (Fig. 4). Then, three tests were conducted at room temperatures to determine the material toughness. The average of the measured CVN energy (CVN = 3.4 ± 0.1 J) and the feature of the fractured surface prove the brittle nature of the specimen material (Fig. 5).

2.2.3. Hardness analysis

The hardness profiles were measured, on a shot–sleeve longitudinal section (Fig. 6 *(b)*) polished until mirror state, from the entry plunger zone to the mold side and from the inner to the outer surface (Fig. 7). These profiles are performed with a Vickers hardness machine using a load of 15 *kg*. The measured profiles reveal that the hardness appears to be constant for all tested samples.

The original hardness of the shot–sleeve as provided by manufacturer technical data–sheet was about 42–44 *HRC*. However, the

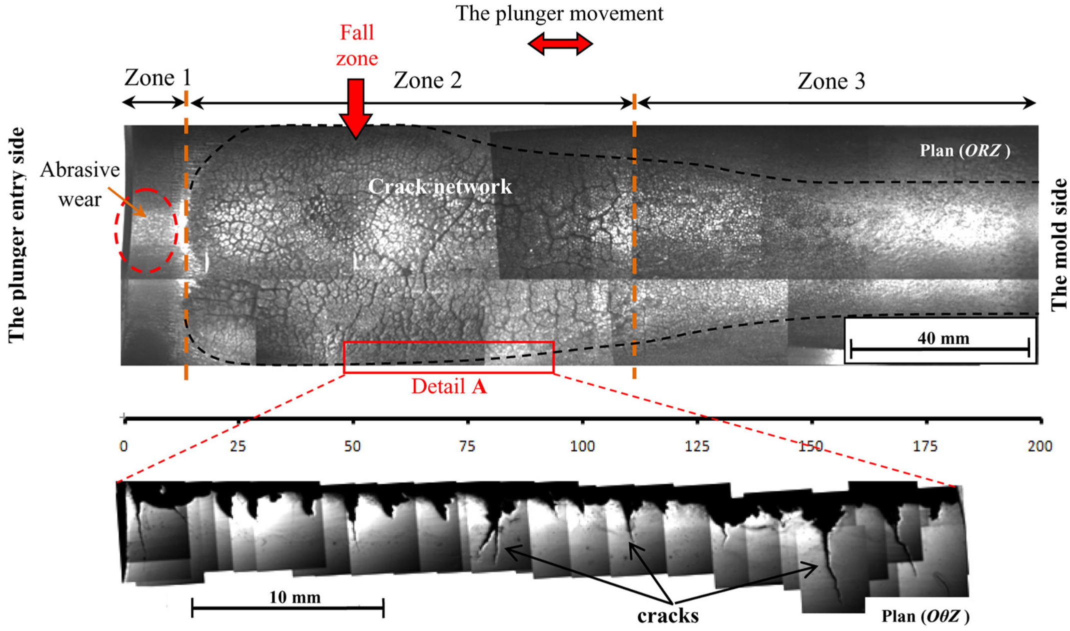

Fig. 9. Shot–sleeve inner surface damage observed with a digital camera.

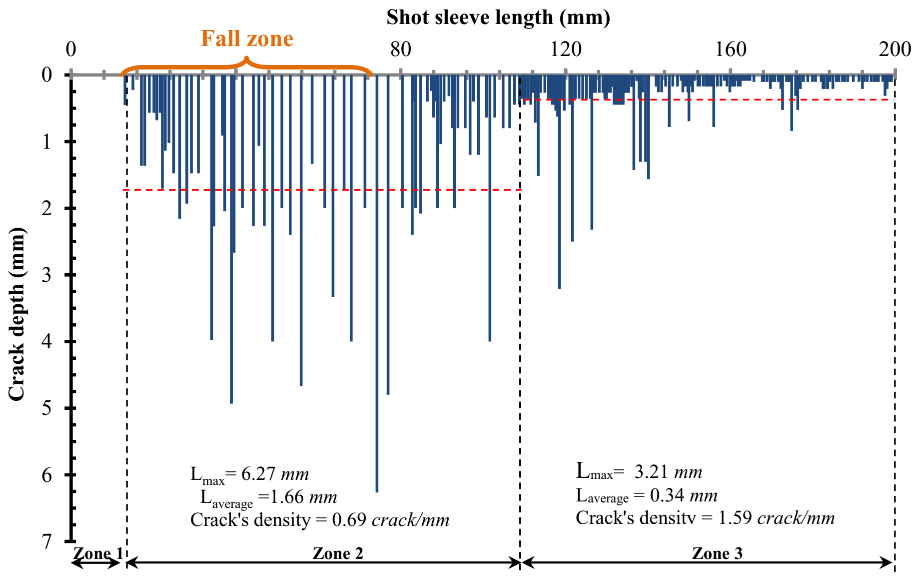

Fig. 10. Crack lengths distribution along the shot sleeve (longitudinal section$\theta = 0$).

average of measured hardness is about of $44.8_{-2.4}^{+3.8}$ *HRC*. This shows that the hardness was remained quasi–constant even after a few thousands of thermal heating and cooling phases (more than 74,000 cycles) and which indicate that the mechanical behaviour of the material is stable (*i.e.* absence of significant cyclic hardening or softening) under service conditions. Furthermore, micro-hardness measurements were performed with a Wilson hardness machine 402MVD using a load of 1 kg at a distance of approximately 400 µm from the inner surface. The average of measured micro-hardness is about $49.8_{-6.4}^{+5.5}$ HRC. This result proves that is no significant increase of the hardness from the heart to the inner surface of the shot-sleeve.

3. Expertise of the damaged shot-sleeves

The metallic structures, which undergo severe cyclic thermo–mechanical loads in service, are typically characterized by the presence of several cracks. These cracks are the most dangerous defects in term of lifetime on which we have to grant a particular attention. In our study, two shot–sleeves damaged in service, supplied by SIAM company, were investigated to determine the

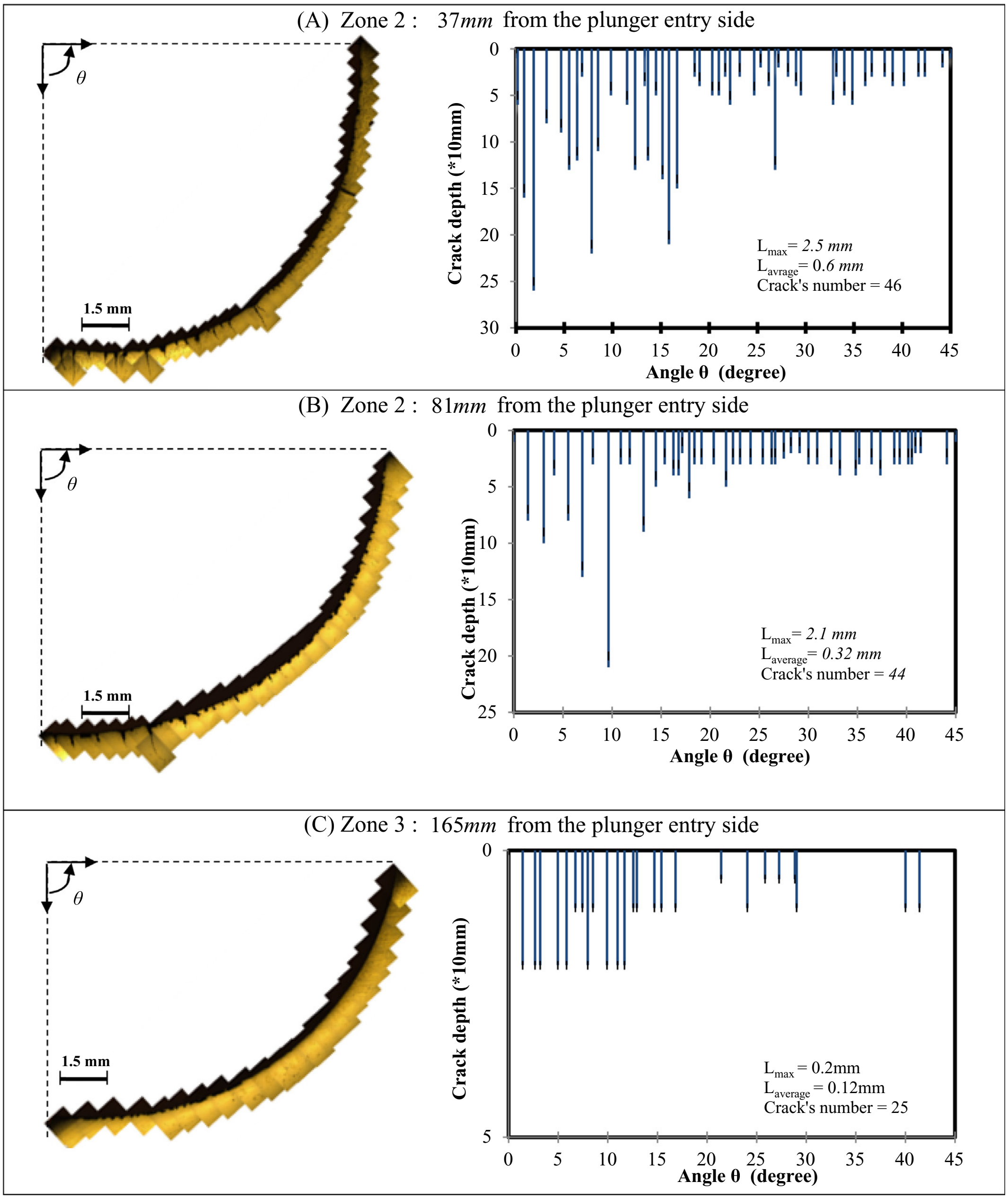

Fig. 11. Crack distribution of damaged shot–sleeve in cross–sections A, B and C.

mechanisms leading to their damages.

The first and the second shot–sleeves have been failed after respectively 46,000 and 74,000 cycles. This corresponds to a quantity of injected molten metal of 18,000 kg and metal

27,000 kg which give an average volume/cycle of 0.39 kg and 0.36 kg, respectively. In addition, only the brass was used as molten metal in these two studied shot-sleeves. According to these previous data, the first shot-sleeve was failed at smaller number of cycles. Which can be explained by the fact that the average of the injected volume per cycle is significantly more important for the first shot-sleeve compared to second one (more than 8.3%).

According to the chemical composition, the microstructure and the preliminary damage observations carried on both shot-sleeves it is obvious that both shot-sleeves are made from the same steel grade (AISI H10) and present the same damage morphology; however, the second shot-sleeve present a more pronounced crack network. As a result, the second shot- sleeve was chosen to conduct the subsequent of the investigation.

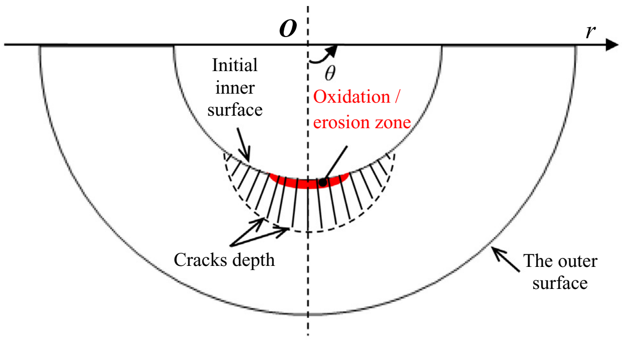

(b) Cracks distribution along the cross section

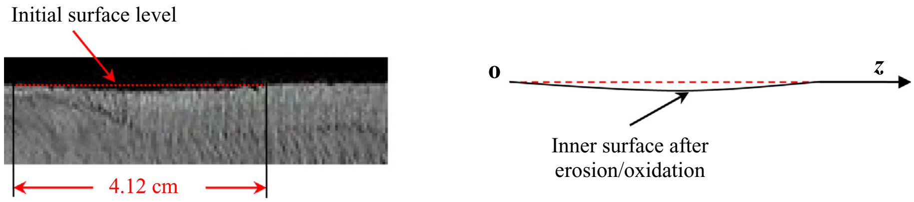

(a) along the axial direction

Fig. 12. Oxidation / erosion effect in the fall zone (Zone 2) of the shot-sleeve.

3.1. Observation of the damaged surfaces

The second shot–sleeve was cut with a wire EDM machine according to their longitudinal direction to examine the integrity of the damaged surface (Fig. 8). After that, the cut–out parts are subjected to a surface cleaning operations: A chemical pickling with an alkaline solution using a dilute nitric acid was performed, at room temperature, to eliminate all traces of oxides. Then, the damaged shot–sleeve surfaces were subjected to a preliminary assessment with a naked eye to identify their major damage features. The examined surfaces (Fig. 9) clearly show the presence of a cracks network on the inner shot–sleeve surfaces.

A finer observations of the shot–sleeve inner side were carried out after a longitudinal cut (Fig. 6 *(b)*). The examination of the damaged surfaces was made using an experimental device equipped with a digital *Baumer®* camera *GIgE* (8 bits). This camera is equipped with a CCD sensor allowing to have a resolution of 1624 × 1236 pixels. Several photos are taken and then assembled by means of Photoshop® software to obtain a large image that cover the entire shot–sleeve examined surface (Fig. 9). This surface reveals the presence of three different zones. The first one is located in the plunger entrance side. It presents a number of scratch according the longitudinal direction which corresponds to abrasive wear caused by the friction between the plunger and the shot–sleeve. The second one corresponds to the first zone which enter in contact with the molten metal ($T = 950\,^{\circ}C$). It undergo cyclic thermal shocks. This zone appears to be the most damaged surface in the shot–sleeve. It presents a dense crack network sign of the thermal fatigue. In addition, the investigation of this zone according to the $O\theta Z$ plan shows that some cracks, after initiation, were propagated in depth along the radial direction (Detail A). The last zone reveals also the presence of a crack network however it is less dense compared to this observed in the *2nd* zone (Fig. 9).

3.2. Quantitative study of the cracks network

In this section, a meticulous investigation on the cracks distribution and density was performed by means of longitudinal and transversal observations (Figs. 10 and 11). The cracks depth according to the axial distance was presented in Fig. 10. It is to be noted that the cracks depth trend along the shot–sleeve follows the Gaussian distribution. Fig. 10 shows that the cracks depth is maximal around the zone *2*, which corresponds to the casting zone (fall zone). This zone is characterized by a maximum crack length and average values of $6.23mm$ mm and $1.66mm$ respectively. In zone 3 the cracks deep is less than those observed in zone *2* nevertheless their density is more pronounced (*i.e.* $1.59 crack/mm$ in zone 3 against $0.69 crack/mm$ in zone *2*). The presence of the shielding effect between neighbouring cracks existing in zone *2* cause the propagation slows down of the smaller cracks and only a few of the biggest ones continue to propagate. Such a phenomenon was observed in many applications in which the thermal fatigue was the main cause of damage [19–20,28].

The cracks depth investigation from the centre of shot–sleeve ($\theta = 0^{\circ}$) to the shot–sleeve horizontal plane ($\theta = 45^{\circ}$) for every shot–sleeve cross–sections A, B and C (Fig. 11). It is obvious that the maximal depths are sited at the level of the zone of casting. This result can be explained by thermal fatigue, oxidation and erosion by the molten brass flow which results in removal of superficial layer.

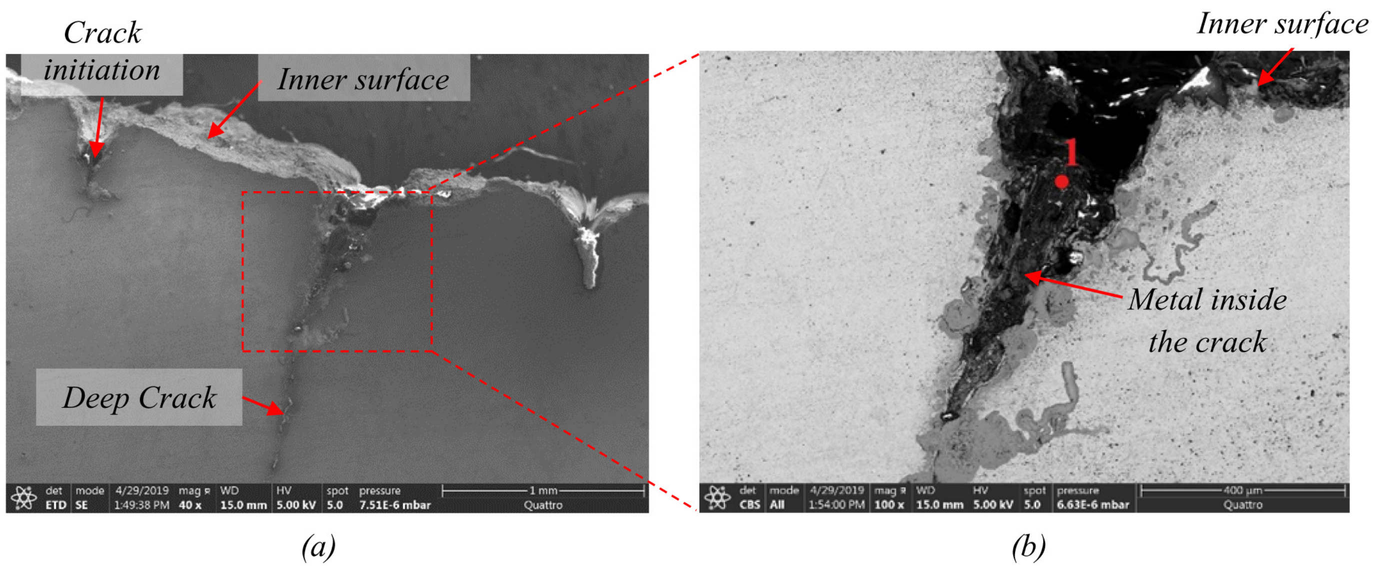

Fig. 13. SEM observation of a damaged shot sleeve cross-section: (a) Short (initiation) and deep crack, (b) Zoom on the examined crack with EDS (point 1).

Table 4
The chemical composition inside crack area (EDS).

	Fe	Cu	Zn	O	Si	S	Cr	Mo
Point 1	5.61	57.03	24.09	1.58	0.13	0.32	0.39	0.77

The initial level of the shot–sleeve casting zone (cited in zone 2) was decreased probably due to oxidation and erosion effects as shown in Fig. 12. The cracks situated surroundings the shot–sleeve centre (near $\theta = 0^{\circ}$) are in reality longer compared to their effective length due to the small decrease of the shot sleeve inner surface level produced after the oxidation / erosion effect. Others micro cracks are totally removed what favoured the propagation of persistent cracks because the motive force was located in them, is confirmed by previous research [1,29].

In addition, in order to more understand the mechanisms leading to the shot sleeve failure, a sample of the cross-section surface was examined using SEM (Fig. 13) and Energy Dispersive X-ray Spectroscopy (EDS) to identify the chemical composition of the metal inside cracks (points 1 in Fig. 13 *(b)*) (Table 4). According to Fig. 13 *(a)*, the cracks tend to propagate perpendicular to the damaged surface. The initial growth of thermal fatigue cracks is facilitated by an oxidation attack on the crack surface, which forms the Fe, Cu, Zn, Cr, Mo, Si and O rich layer (Table 4). The presence of brass and oxides, in the cracks increases plastic yield ($Rp_{0.2}$) and compressive stresses during the heating phase of the thermal cycle [30]. As a result, the tensile stress is further increased during the cooling phase and can leads to the acceleration of the crack growth rate. In addition, the tensile stresses applied on the shot-sleeve inner surface during the cooling phase combined with the erosion phenomenon caused by the molten brass fall in the second zone leads to a local failure, which promote the opening of thermal cracks [13]. These cracks act as channels allowing oxygen to penetrate down to the crack tip area and oxidize both shot sleeve and the filling material. Solidified particles down on the crack act as an obstacle for its closer and the size of the crack openings in the filling material indicates the amount of brass that will fill the crack during the next cycle [20].

4. Conclusions

The investigation of a failed shot–sleeves used in high pressure brass die–casting was carried out in this study. The failed shot-sleeve was at first investigated by the determination of chemical composition, microstructures and hardness. The cracks surface network, observed at the inner surfaces of all the examined shot–sleeves, were shown the presence of three different zones: *(i)* entered piston, *(ii)* entrance of the molten metal and *(iii)* exit of the molten metal. These zones differ by their feature, cracks network density and depths. The longitudinal section shows that the second zone possess the maximum values of cracks depth. In addition, the cross section shows that the maximal cracks length are situated in the vicinity of the shot–sleeve centre ($\theta \approx 0^{\circ}$). According to the foregoing discussion it is clear that thermal fatigue is the first cause of shot–sleeve damage. However other phenomena like oxidation and erosion of the shot-sleeve inner surface cause the increases of the damage rate mainly in the casting zone (fall zone).

Acknowledgements

The authors would like to thank Mr. H. Ammar the Head manager of SIAM for fruitful discussions about shot–sleeves failure mode, the material support and for chemical analysis of the studied steel samples.

References

[1] B. Miquel, S. Jean, S. Le Roux, P. Lamesle, F. Rézaï-Aria, Heat checking of hot work tool steels, Proceedings of the 9th International Conference on Temperature-fatigue Interaction, 2002, pp. 185–193.
[2] A. Srivastava, V. Joshi, R. Shivpuri, Computer modeling and prediction of thermal fatigue cracking in die-casting tooling, Wear 256 (2004) 38–43.
[3] A. Persson, S. Hogmark, J. Bergström, Thermal fatigue cracking of surface engineered hot work tool steels, Surf. Coat. Technol. 191 (2005) 216–227.
[4] S. Le Roux, F. Medjedoub, G. Dour, F. Rézaï-Aria, Role of heat-flux density and mechanical loading on the microscopic heat-checking of high temperature tool steels under thermal fatigue experiments, Int. J. Fatigue 51 (2013) 15–25.
[5] S. Jean, B. Miquel, S. Le Roux, F. Rézaï-Aria, An investigation on heat checkingof hot work tool steels, Proceedings of the 5th International Conference on Tooling, Tool Steels of the Next Century, University of Leoben, Austria, September 29–October 1, 1999, pp. 185–193.
[6] F. Medjedoub, G. Dour, F. Rezaï-Aria, P. Hairy, Endommagement par faïençage des moules de fonderie sous pression en fatigue thermique: origines, mécanismes et approches, Fonderie Fondeur d'Aujourd'hui 244 (2005) 22–37 (in French).
[7] L.A. Norström, M. Svensson, N. Öhrberg, Thermal fatigue behaviour of hot work tool steels, Metals Technol. 10 (1981) 376–381.
[8] A. Persson, S. Hogmark, J. Bergström, Simulation and evaluation of thermal fatigue cracking of hot work tool steels, Int. J. Fatigue 26 (2004) 1095–1107.
[9] R. Danzer, F. Sturm, A. Schindler, W. Zlepping, Thermal fatigue cracks in pressure die casting dies, Giessereipraxis 19/20 (1983) 287–297.
[10] B. Kosec, L. Kosec, J. Kopač, Analysis of casting die failures, Eng. Fail. Anal. 8 (2001) 355–359.
[11] R.W. Neu, H. Sehitoglu, Thermo-mechanical fatigue, oxidation, and creep. Part 1: damage mechanisms, Metal Trans. A. 20A (1989) 1755–1767.
[12] P. Panjan, M. Čekada, R. Kirn, M. Soković, Improvement of die-casting tools with duplex treatment, Surf. Coat. Technol. 180 (2004) 561–565.
[13] D. Mellouli, N. Haddar, A. Köster, H.F. Ayedi, Hardness effect on thermal fatigue damage of hot-working tool steel, Eng. Fail. Anal. 45 (2014) 85–95.
[14] J. Tidlund, Heat checking in hot work steels, 2nd International Colloquium on Tool Steels for Hot Working, Saint Etienne (France), 1977, pp. 1–38.
[15] L. Cser, M. Geiger, K. Lange, J.A.G. Kals, M. Hänsel, Tool life and tool quality in bulk metal forming, Proc. Inst. Mech. Eng. 207 (1993) 223–239.
[16] A. Skumavc, J. Tušek, A. Nagode, D. Klobčar, Thermal fatigue study of tungsten alloy WNi28Fe15 cladded on AISI H13 hot work tool steel, Surf. Coat. Technol. 285 (2016) 304–311.
[17] C.M.D. Starling, J.R.T. Branco, Thermal fatique of hot work tool steel with hard coatings, Thin Solid Films 436 (1997) 308–309.
[18] S. Malm, L.A. Norström, Material-related model for thermal fatigue applied to tool steels in hot work applications, Metal Sci. (September) (1979) 544–550.

[19] A. Ktari, N. Haddar, H.F. Ayedi, Fatigue fracture expertise of train engine crankshafts, Eng. Fail. Anal. 18 (2011) 1085–1093.
[20] D. Mellouli, N. Haddar, A. Köster, H.F. Ayedi, Thermal fatigue failure of brass die-casting dies, Eng. Fail. Anal. 20 (2012) 137–146.
[21] A. Srivastava, V. Joshi, R. Shivpuri, R. Bhattacharya, S. Dixit, A multilayer coating architecture to reduce heat checking of die surfaces, Surf. Coat. Technol. 163 (2003) 631–636.
[22] D. Klobčar, L.K.J. Kosec, B. Kosec, J. Tušek, Thermo fatigue cracking of die casting dies, Eng. Fail. Anal. 20 (2012) 43–53.
[23] M. Fazarinc, T. Muhič, G. Kugler, M. Terčelj, Thermal fatigue properties of differently constructed functionally graded materials aimed for refurbishing of pressure-die-casting dies, Eng. Fail. Anal. 25 (2012) 238–249.
[24] S. Jean, B. Miquel, S. Leroux, F. Rézaï-Aria, An investigation on heat checking of hot work tool steels, in: F. Jeglitsch, R. Ebner, H. Leitner (Eds.), Tool Steels of the Next Century, Proceedings of the 5th International Conference on Tooling, University of Leoben, Leoben, Austria, 1999, pp. 185–193.
[25] R. Reynoldson, Die Casting Tools Manufactured From H13 Hot Work Tool Steels, Die Casting and Technology, (September 1998), pp. p39–p49.
[26] H. Bayrakçeken, S. Tasgetiren, F. Aksoy, Failure of a single cylinder engines crank shafts, Eng. Fail. Anal. 14 (2007) 725–730.
[27] R. Lévêque, Données numériques sur les aciers à outils, Techniques de l'Ingénieur : Etude et propriétés des métaux, M 332 V1, 1995, pp. 1–37 (in French).
[28] V. Maillot, A. Fissolo, G. Degallaix, S. Degallaix, Thermal fatigue crack networks parameters and stability: an experimental study, Int. J. Solids Struct. 42 (2005) 759–769.
[29] F. Medjedoub, S. Le Roux, G. Dour, F. Rézaï-Aria, Effect of local stress on the heat-checking morphology in high temperature tool steels under thermal fatigue: transition from multi-axiality to uniaxiality, Mech. Mater. 69 (2014) 159–172.
[30] D. Klobčar, J. Tušek, B. Taljat, Thermal fatigue of materials for die-casting tooling, Mater. Sci. Eng. A 472 (2008) (2008) 198–207.